

# STATISTICAL ANALYSIS OF A SODA LIME GLASS THERMAL SHOCK RESISTANCE

ZAHRA MALOU<sup>\*(\*\*)</sup>, #MOHAMED HAMIDOUCHE<sup>\*(\*\*)</sup>, NOUREDDINE BOUAOUADJA<sup>\*\*</sup>, GILBERT FANTOZZI<sup>\*\*\*</sup>

<sup>\*</sup>Unité de recherche Matériaux Emergents, Université Ferhat Abbas 19000 Sétif, Algérie

<sup>\*\*</sup>Laboratoire des Matériaux Non Métalliques, Institut d'Optique et Mécanique de précision,  
Université Ferhat Abbas 19000 Sétif, Algérie

<sup>\*\*\*</sup>MATEIS, UMR CNRS 5510, INSA de Lyon, 69621 Villeurbanne, France

#E-mail: mhamidouche@univ-setif.dz

Submitted March 24, 2011; accepted July 18, 2011

**Keywords:** Soft thermal shock, Severe thermal shock, glass, Mechanical strength, Weibull analysis

*Comparatively to the as received soda lime glass samples, the strength distribution after thermal shocks showed the appearance of a second branch in the Weibull curves. This branch is observed for temperature differences ( $\Delta T$ ) equal or higher than the critical temperature difference ( $\Delta T_c$ ) for both water and motor oil cooling baths. The dispersion is more spread out in these two baths in comparison with the olive oil bath probably because of more pronounced slow crack growth effect. The Weibull modulus varies according to the used cooling bath and the considered temperature difference.*

*In the case of thermal shock caused by air blast cooling at  $T = 20^\circ\text{C}$ , a bimodal distribution is observed for only the critical state. The initial cracking time, obtained by acoustic emission, corresponds to the unstable propagation of the most critical defect. The number of cracks induced by thermal shock is proportional to the number of acoustic events.*

## INTRODUCTION

Brittle materials and glass in particular are susceptible to failure under the effect of sudden temperature variations. The amplitude of the critical temperature difference is related to the initial state, the geometry and the dimensions of the tested material [1, 2]. The reliability of these materials is determined by two important factors: the fracture strength and the Weibull modulus. When strength tests are carried out on a set of similarly prepared samples, dispersion on the obtained strength values is observed.

The strength depends on the material surface quality reflecting the size and the density distribution of the defects initiating fracture [3]. These defects exert a great influence on the fracture characteristics [4]. Glass has the peculiarity to contain a great number of surface flaws.

To predict fracture, knowledge solely of the results given by elastic linear fracture mechanics and sub-critical crack growth on the preexisting defects in the material is insufficient [5]. The use of theories based on the statistical nature of brittle fracture is essential for estimating the probable failure [2, 6]. It is thus necessary to seek methods providing statistical laws based on a relatively low number of experimental data such as the developed Weibull analysis [7].

The equation of the cumulated fracture probability proposed by Weibull has the following form:

$$P = 1 - \exp \left[ - \left( \frac{\sigma}{\sigma_{0_1}} \right)^{m_1} \right] \quad (1)$$

where  $\sigma$  is applied stress,  $\sigma_0$  stress for which the probability of rupture is 0.63 for a unit volume. It is known as normalization stress and does not have any physical significance.  $m$  is Weibull modulus expressing the dispersion degree of the fracture data. The Weibull modulus represents also the homogeneity of the defects distribution.

In situations where two or more populations of defects exist in the sample, and control the fracture stress distribution, the strength distribution does not provide a simple Weibull distribution where the direct application of Equation (1) is used. We rather have a non-linear form. In this analysis, it is assumed that there are only two flaws populations. The new equations which represent the two populations are given respectively by [8]:

$$S_1 = \exp \left[ - \left( \frac{\sigma}{\sigma_{0_1}} \right)^{m_1} \right] \quad (2)$$

$$S_2 = \exp \left[ - \left( \frac{\sigma}{\sigma_{0_2}} \right)^{m_2} \right] \quad (3)$$

where  $m_1$ ,  $m_2$ ,  $s_{o1}$ ,  $s_{o2}$  are respectively the Weibull modulus and the normalization stress associated to the flaws population 1 and 2.

$S_1$  and  $S_2$  are the survival probabilities associated to the defects of population 1 and 2 respectively.

The total survival probability  $S$  is function of the localisation of the flaws (inner or surface flaws) and of the defect nature (intrinsic or extrinsic flaws). In the present work, we considered two possible cases: a partially concurrent distribution and an exclusive one.

For a partially concurrent case, the defects of population 1 are common to all the samples. If a fraction "a" of the samples contains only this type of flaws, the remaining portion of the samples (1- a) contains additionally a second type of defects. Both populations 1 and 2 are present in the remaining portion. The total survival resulting probability is:

$$S = \alpha \cdot S_1 + (1 - \alpha) S_1 \cdot S_2 \quad (4)$$

where "a" is a mixed parameter.

For an exclusive distribution case, a fraction a of the samples contains only the defects of population 1; the remaining portion of the samples (1- a) contains only the defects of population 2. The total survival probability has the following form :

$$S = \alpha S_1 + (1 - \alpha) S_2 \quad (5)$$

During thermal shock, for a bi-dimensional stress state, the induced thermal stress on the material surface has the following form:

$$\sigma = \psi(\beta) \cdot \left( \frac{E\alpha\Delta T}{1-\nu} \right) \quad (6)$$

where  $E$  - Young modulus,  $\alpha$  - linear thermal expansion coefficient,  $\Delta T$  - sample temperature difference between the initial and final state,  $\nu$  - poisson's ratio.

With  $0 \leq \psi(\beta) \leq 1$   $\beta$  is defined as:

$$\beta = \frac{h \cdot l}{k} \quad (7)$$

where  $h$  is the heat transfer coefficient,  $l$  the characteristic dimension of the sample and  $k$  the thermal conductivity of the material.

Under the same thermal shock tests conditions, some samples break while others do not [9]. Manson and Smith [10] introduced the statistical aspect of the thermal shock using Weibull formulation.

The fracture conditions of a thermal shock can be reached, not when the surface stress reaches a maximum, but rather when the fracture probability is maximum [10]. The statistical aspect of the thermal shock results is evident, particularly for severe cases. A linear correlation between this aspect and the damage parameters, using a statistical analysis, was proposed by Volkov et al. [11]. As glass strength is probabilistic in nature, the statistic aspect of the thermal shock strength should logically be considered [12].

## EXPERIMENTAL

A silica-soda lime glass was used in this work. Its chemical composition contains mainly: 72.2 %  $\text{SiO}_2$ , 15 %  $\text{Na}_2\text{O}$ , 6.7 %  $\text{CaO}$ , 4 %  $\text{MgO}$ , 1.9 %  $\text{Al}_2\text{O}_3$  and 0.2 % impurities. Its usual characteristics obtained at ambient temperature are: Linear expansion coefficient  $\alpha = 8.1 \times 10^{-6} \text{ }^\circ\text{C}^{-1}$ , Elastic modulus  $E = 72 \text{ GPa}$ , Transition temperature  $T_g = 550 \text{ }^\circ\text{C}$  and Toughness  $\text{KIC} = 0.75 \text{ MPa}\cdot\text{m}^{1/2}$ .

After the cutting operation, all the samples were rectified to the needed dimensions. Two thicknesses (3 and 4 mm) with ( $15 \times 50 \text{ mm}^2$ ) sample surface were used for the soft thermal shock. The 4-mm thickness was only used for the severe shock and the surface in this case is equal to ( $6 \times 50 \text{ mm}^2$ ). The edges of the samples were chamfered by grinding. This operation is necessary to limit their effect during the mechanical and thermal shock tests. The samples were annealed at  $550^\circ\text{C}$  during 30 min, in order to eliminate residual stresses.

The device used for severe thermal shock tests is composed of a furnace, a sample holder and a cooling liquid container (oil or water).

In the case of the soft thermal shock, the tests were carried out using a compressed air blast on samples using the two selected thicknesses.

The device used for soft thermal shock tests is shown in Figure 1. A computer is used for recording the acoustic activity and controlling the device handling operations.

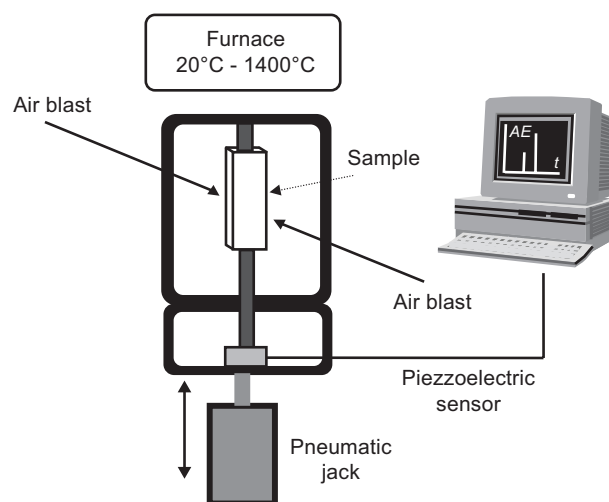


Figure 1. Apparatus for thermal shock tests by air blast.

Each sample was kept in the furnace during 10 min in order to make its temperature uniform. After the thermal shock test, the samples were tested in 4 points bending on an universal testing machine. The distances between the outer ( $l$ ) and inner ( $l'$ ) spans are respectively 10 mm and 35 mm and the used loading rate is of 0.5 mm/min. The fracture stress is given by the following relation:

$$\sigma_r = \frac{3F_r(l-l')}{2b \cdot w^2} \quad (8)$$

where b - sample width, w - sample height,  $F_r$  - fracture load.

The critical temperature variation was determined for each type of test. The different undertaken thermal shock tests are shown in Table 1.

RESULTS AND DISCUSSION

First of all, we show in Figure 2 an example of calculation using the two tested methods (Least squares test and chi2 test). The curves represent the survival probability Ps according to the fracture stresses for the just critical case for samples shocked in a motor oil bath. The Ps probabilities as well as the Weibull's parameters are calculated using these two methods. We noticed that the chi2 test is more appropriate if we consider the closeness of the curves obtained from the experimental and theoretical values.

The different parameters are calculated with the least square method and the chi2 test for the partially concurrent distribution (Equation (5)). Good agreement

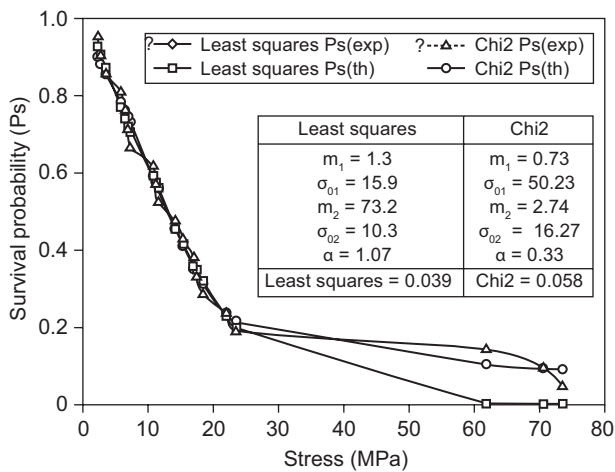


Figure 2. Variation of survival probability Ps versus stress  $\sigma$  for prismatic samples (e = 4 mm) shocked in oil for just critical shock (350°C and tested in 4 points bending).

with the experimental data is obtained in this case and chi2 test.

Figure 3 represents the dispersion of the fracture stresses obtained on samples shocked in water at 20°C. The tests were carried out for different temperature variations:  $DT = 0^\circ C$  (no shock),  $DT = 120^\circ C$  (sub-critically shock),  $DTc = 150^\circ C$  (critical shock) and  $DT = 180^\circ C$  (over critical shock).

At the beginning for the non shocked samples, the dispersion is lower and unimodal. For the samples under, just and over critically shocked conditions, the distribution moves towards the low values of  $\sigma_r$  and becomes rather bimodal. A part of the samples is damaged by thermal shock while another part remains as it was. This is explained by the existence of two defect populations: the original flaw population which was not affected by the thermal shock (the high-strength) and a flaw population modified by thermal shock (lower-strength) [13]. In the under critical and over critical cases, the rather weak proportion (a) of naturals defects leads to larger dispersion. At the just critical temperature, the proportions disparity increases.

For low stresses, the branches are characterized by slopes noted  $m_2$  (defects modified by thermal shock). The second branches (high values of fracture stress)

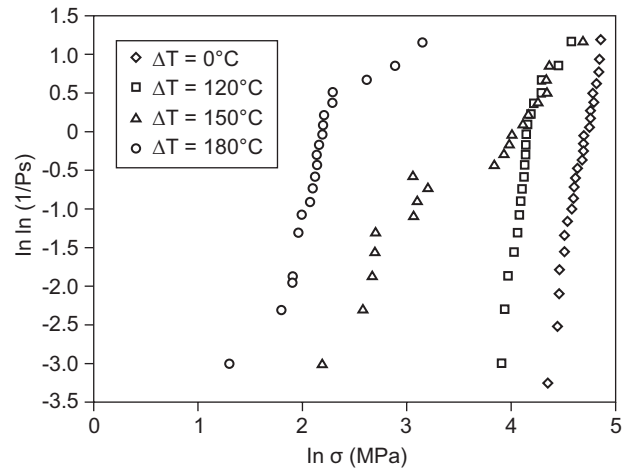


Figure 3. Variation of  $\ln \ln (1/Ps)$  versus  $\ln (\sigma)$  for prismatic samples (e = 4 mm) shocked in water for different temperature variations and tested in 4 points bending.

Table 1. Conditions realised during thermal shock tests.

	Specimen thickened				
	e = 4 mm			e = 3 mm	
Temperature differences	Water cooling	Motor oil cooling	Olive oil cooling	Compressed air cooling	Compressed air cooling
$\Delta T = 0$	No shock	No shock	No shock	No shock	No shock
$\Delta T < \Delta Tc$	120°C	300°C	-	190°C	240°C
$\Delta T = \Delta Tc$	150°C	350°C	270°C	220°C	270°C
$\Delta T > \Delta Tc$	180°C	400°C	-	-	280°C to 320°C

are characterized by Weibull modulus  $m_1$  (natural flaws). In this low stresses case, during the samples heating, primary flaws can be closed or healed and a stress relaxation occurs. This leads to more resistant samples and higher fracture stresses. The values of the normalization stresses ( $s_{01}$  and  $s_{02}$ ) respectively for the first and the second branch decrease when the applied temperature differences increase. We notice that independently of the type of cooling bath used, the larger dispersion corresponds to the natural flaws (generally  $m_1$  lower than  $m_2$ ), as shown in Table 2.

A clear disparity in the dispersions according to the applied temperature difference can be noticed. From a statistical point of view, it is not easy to make a direct comparison between thermal shock and mechanical tests. In the case of the mechanical stresses, the applied load varies from zero up to a maximal value, taking into account the solicited surface between the used supports (inner span). According to Kamiya et al. [14], the stress distribution is uniform on the entire surface in the case of thermal shock.

During cooling, the surface cools faster than the bulk material. As a result, material near the surface attempts to shrink while being constrained by the interior of the material which is at higher temperature. Such constraint causes tensile stresses in the surface region. The fracture origin is controlled by the extension of small flaws which are dispersed in specimen's surface. These cracks are responsible of the failure initiating during thermal choc (Figure 4).

Rogers et al. [9] found that the number of the damaged samples is larger when the thermal shock is more severe. Ainsworth and Moore [15] reported that the strength data dispersion decreased with increase in the density of the induced flaws. This shows that the critical temperature difference is not a constant value. It can be well described by a statistical distribution. On the other hand, it is assumed by Danzer et al. [16] that the strength depends on the size of the largest (or critical) defect that varies on each specimen. Therefore, the strength of a ceramic material cannot be described uniquely by a single value. A strength distribution function is necessary and a large number of specimens are required to characterize it.

The cracking mechanism of the samples shocked in an oil bath is different from those shocked in water. In the oil bath, cracking is single whereas in water, crack branching occurs. Kamiya [14, 17] reported that the heat transfer coefficient "h" is lower in the oil bath case. A bimodal distribution is also observed after thermal shock (Figure 5). In the over-critical case, the populations of defects present the same dispersion and almost have equal proportions. In comparison with the results obtained for by quenching into water, the values of Weibull modulus in the oil bath are slightly lower, particularly the  $m_2$  values (Table 2). This behavior can be explained by the fact that single cracking is normal to the sample surface. During bending tests, these defects are solicited in the opening mode (in tension), leading thus to lower and dispersed fracture stress values. This is not the case for thermal shock tests in water where the same crack presents several ramifications. Ashizuka [13] in his work on a borosilicate glass, shocked in distilled

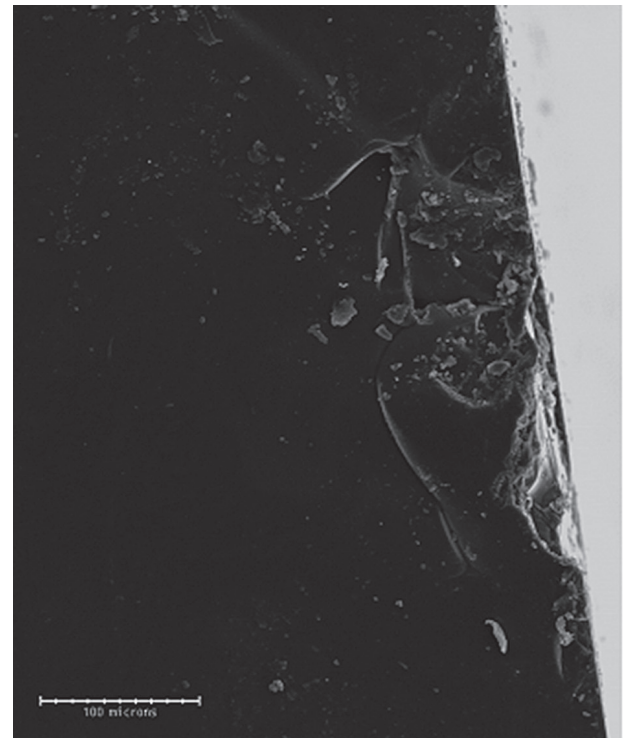


Figure 4. Natural superficial initiating crack.

Table 2. Results of the statistical parameters of as received samples and of samples thermally shocked in water and oil.

Tests condition	Motor oil cooling bath			Olive oil cooling bath	Water cooling bath			With out thermal shock
	400	350	300		270	180	150	
$\Delta T$ (°C)								0
$m_1$	2.39	0.73	4.69	5.9	1.91	2.40	5.00	6.95
$m_2$	2.38	2.74	7.35	19	14.65	10.65	18.30	–
$\sigma_{01}$ (MPa)	23.07	50.23	64.72	95.3	16.61	67.53	85.86	112.62
$\sigma_{02}$ (MPa)	6.11	16.27	29.42	11	8.74	14.83	63.28	–
$\alpha_1$	0.41	0.33	0.69	0.82	0.30	0.70	0.27	1
Chi 2	0.039	0.058	0.036	0.034	0.016	0.083	0.024	0.078

water and liquid nitrogen, showed that similar contrasted distributions were related to the apparent existence of slow crack growth during the thermal shock. This effect is greatly enhanced by testing in water, a condition that promotes further the slow crack growth by stress corrosion.

The results obtained with the olive oil bath for critical shock (270°C) are represented in Figure 5 with those of the water bath and the motor oil bath. The just critical temperature differences found in the case of the olive oil bath and the strengths are lower than those obtained for the other cooling baths. The dispersion for the thermal shock by quenching into water and motor oil are more spread out. We think that, unlike for the water bath, there is no sub-critical crack growth in the olive oil bath. Weibull's modulus values are however, higher.

For the cooling by air blast, it can be noticed that the dispersion is more important around the critical case. The kind of cooling bath has a considerable effect on Weibull

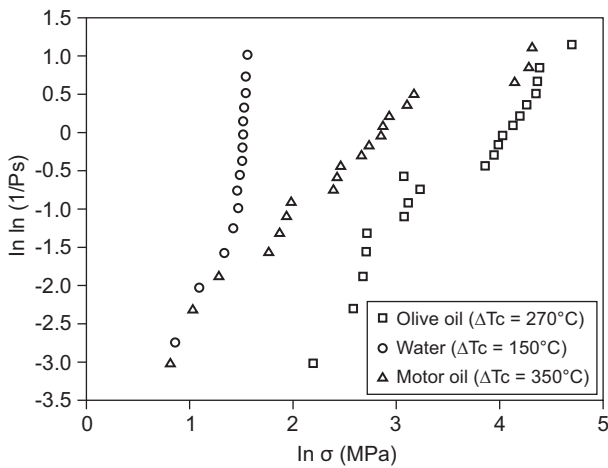


Figure 5. Variation of  $\ln \ln (1/P_s)$  versus  $\ln (\sigma)$  for prismatic samples ( $e = 4 \text{ mm}$ ) shocked in motor oil, olive oil and water for different temperature variations and tested in 4 points bending.

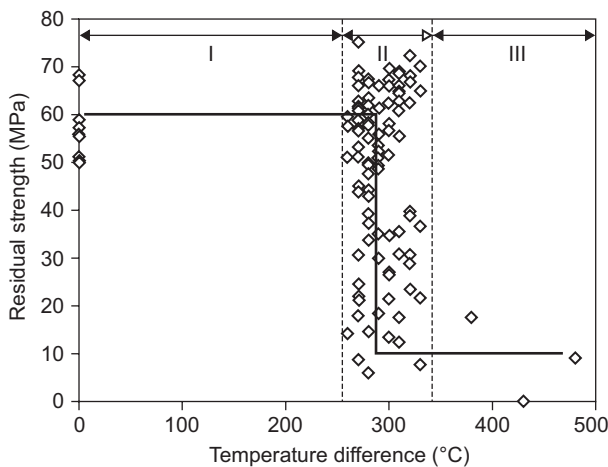
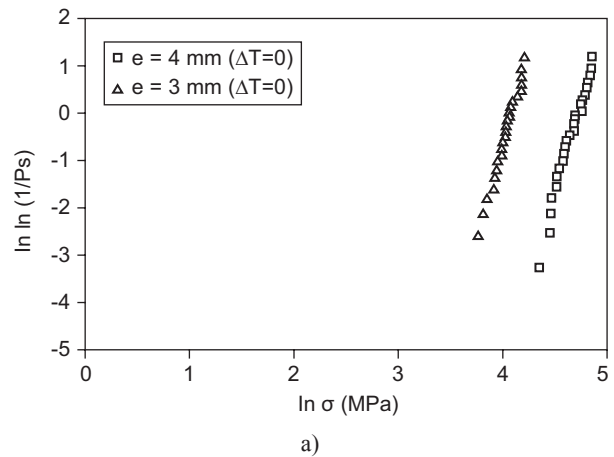


Figure 6. Residual strength versus temperature difference  $\Delta T$  for an as received glass with 3 mm thickness (soft thermal shock by air blast).

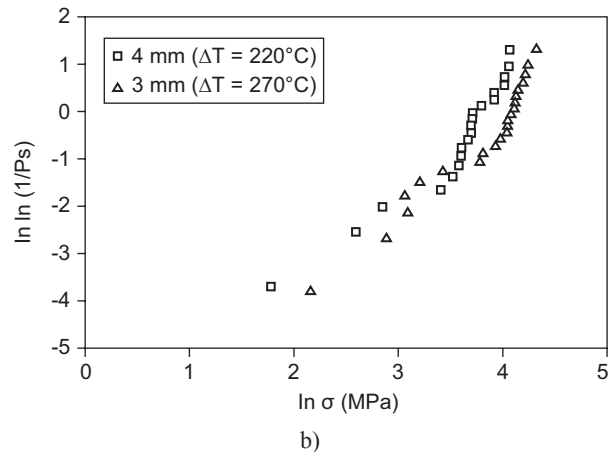
modulus values. Residual strength variation according to the temperature difference in this case for an as received 3 mm thickness sample is presented in Figure 6. There is no change in the mechanical strength until  $\Delta T = 270^\circ\text{C}$ . Beyond this gradient, a decrease is observed. For  $\Delta T > 330^\circ\text{C}$ , all the samples are completely damaged. Between these two difference temperatures, a significant number of samples present a mechanical strength similar to that of the initial value whereas it falls considerably for the remaining others.

The evolution of the residual strength was subdivided by Joong Hyun Lee et al. [18] in into three areas noted I, II, III. In the first area there is no change in the initial strength. In the second area, the mean residual strength decreases gradually and finally in the third area, all the samples undergo a catastrophic damage with a brutal fall of the strength. The authors affirm that it is more interesting to study the second area results. On the basis of this suggestion, only this domain was considered.

In the case of a thermal shock by air blast cooling, the just critical shock  $\Delta T = \Delta T_c$ , two branches for the two thicknesses are observed (Figures 7 and 8). This justifies the presence of two defects population corresponding to



a)



b)

Figure 7. Variation of  $\ln \ln (1/P_s)$  versus  $\ln (\sigma)$  for different thicknesses ( $\Delta T = 0$ ) and shocked by air blast ( $\Delta T = \Delta T_c$ ).

the two slopes on Weibull plots. For the under critical case, it represents the pristine flaw population without the thermal shock influence [13]. For this type of cooling, the values of  $m_1$  for the two thicknesses are considerably smaller than  $m_2$  values.

Acoustic emission is used to detect the events due to the sudden propagation of the cracks. The appearance of the first acoustic emission peak during a very short time reveals the fast propagation of the most critical crack (Figure 9). This event allows us to determine the critical temperature difference for each thickness. The acoustic emission technique does not provide a detection of the stable crack growth.

According to Kingery [19], the critical temperature difference is that for which a first crack is visible. This difference allows determining the first parameter  $R$  of thermal shock resistance. For the 3 mm thickness glass, no acoustic activity was recorded before  $\Delta T = 270^\circ\text{C}$ . The first acoustic emission peak of maximum amplitude appears for a 1245 ms duration (Figure 9). This time corresponds to the sudden propagation of the most critical natural flaw. A second peak of the same intensity and further weaker peaks follow, revealing the onset of the propagation.

On the other hand, a large dispersion appears particularly for the thermal shocks close to the critical shock ( $\Delta T_c = 270^\circ\text{C}$ ). In order to confirm this result, the variation  $\ln \ln(1/(1 - P_s))$  versus  $\ln(t)$  is also given

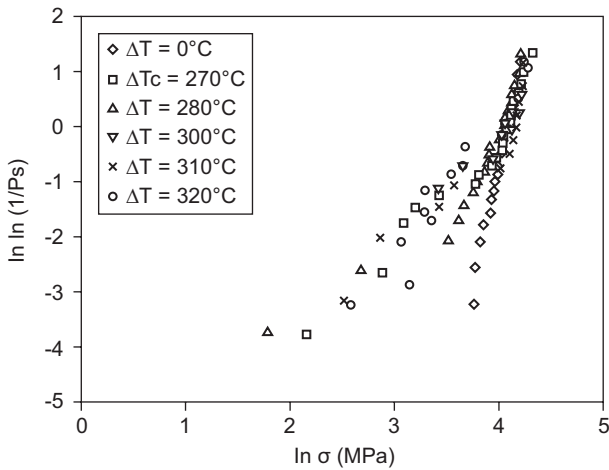


Figure 8. Probability of rupture according to  $\ln \ln(\sigma)$  for various temperature differences  $\Delta T$  for 3 mm glass thickness thermally shocked by air cooling.

in Figure 10. This function indicates that the fracture probability occurs at the moment corresponding to the first acoustic emission peak. All the lines are unimodal and the time dispersion of acoustic emission is the same for all the temperature differences. Weibull modulus values are lower than those found in the case of the mechanical strength distribution values (Table 3), but closer to the  $m_2$  value found for the most over critical shock ( $310^\circ\text{C}$ ). Similarly to the critical temperature variation, the time evolution will be well described by a Weibull statistical function in the area announced by Joong Hyun Lee et al. [19].

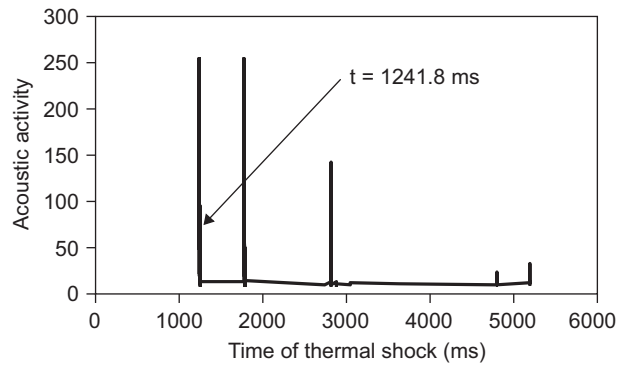


Figure 9. Acoustic activity versus time for an as-received glass with a thickness  $e = 3$  mm, shocked by air blast at a temperature difference  $\Delta T = 270^\circ\text{C}$ .

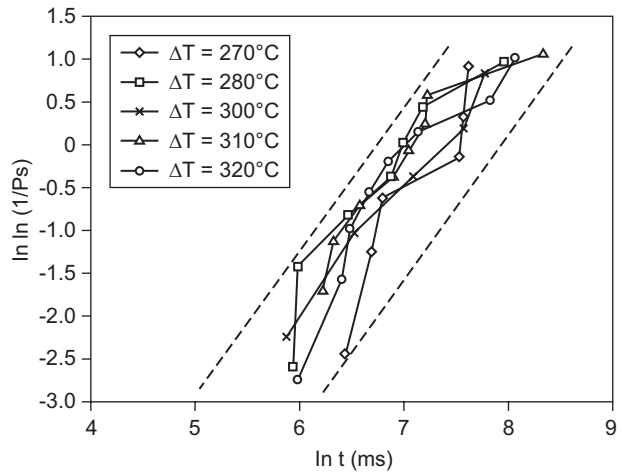


Figure 10. Fracture probability versus acoustic emission time  $t$  for various thermal shocks for 3 mm thickness glass (soft thermal shock by air-cooling).

Table 3. Weibull modulus for specimen thermally shocked by air at different temperature differences (thickness = 3 mm) determined by measured mechanical strength and acoustic emission times when the first crack appears.

Temperature differences $\Delta T$ ( $^\circ\text{C}$ )		0	270	280	300	310	320
By residual mechanical strength	$m_1$	7.6	6.37	9.47	8.97	16	12.2
	$m_2$	–	5.29	4.46	3.11	1.7	4.9
By acoustic emission times	$m$	59.3	62.14	61.42	64.36	66.3	69.1

## CONCLUSION

Throughout the various thermal shock tests carried out on a soda lime glass under various experimental conditions, it appears that the critical temperature difference DTc can not be defined by a distinct singular value. Its variation can adequately be described by Weibull statistical model.

Independently of the used cooling bath type, it clearly appears that the dispersion becomes larger when the critical state is approached. This dispersion is also characterized by the appearance of a second population (bimodal Weibull's curves) related to the severity of the undergone thermal shock. For the thermal shock caused by a compressed air blast cooling, more important strength is obtained for the smallest thickness.

The first peak obtained by acoustic emission response corresponds to the sudden propagation of the most critical pre-existent flaw. Like the critical temperature difference, this time is well described by Weibull statistical distributions.

## Acknowledgments

*The Authors thanks M. R'Mili and P. Reynaud for their assistance in the statistical analysis.*

## References

1. Hasselman D.P.H.: J. Am. Ceram. Soc. 52, 600 (1969).
2. Hasselman D.P.H.: Mat. Sci. and Engin. 71, 251 (1985).
3. Jurgen S., Nils C., Jurgen R. : J. Europ. Ceram. Soc. 17, 727 (1997).
4. Lamon J. : Revue de Métallurgie, pp. 265-284, February 1995.
5. Chermant J.L. : Presse du CNRS, p.198, Paris 1989.
6. Hasselman D.P.H. in: *Fract. Mec. of Ceram.*, Vol. 11: *R-Curve, Toughness Determination and Thermal Shock* , Bradt (Eds.), 1994.
7. Pollard A., Rivoire C.: Edition Eyrolles p.140, 1971.
8. R'mili M., Shulte C.: Composite Science and Technology 68, 1800 (2008).
9. Rogers W.P., Emery A., Bradt R.C., Kobayashi A.S.: J. Am. Ceram. Soc. 70, 406 (1987).
10. Manson S.S., Smith R.W.: J. Am. Ceram. Soc. 1, 18 (1955).
11. Volkov-Husovic T.D., Jancic R.M., Popovic Z.V.: Engen. Mater. Vols. 132-136, pp. 603- 606, 1997.
12. Wereszczak A., Scheidt R., Ferber R.M., Breder K.: J. Am. Ceram. Soc. 82, 3605 (1999).
13. Ashisuka M., Easler T.E., Bradt R.C.: J. Am. Ceram. Soc. 66, 543 (1983).
14. Kamiya I., Kamigaito O.: J. Mater. Sci. 24, 477 (1989).
15. Ainsworth J.H., Moore R.E.: J. Am. Ceram. Soc. 52, 628 (1968).
16. Danzer R., Lube T. , Supancic P., Damani R.: Advanced Engineering Materials 10, 275 (2008).
17. Kamiya N., Schneider G.A., Petzow G. (Eds.), 1993, pp. 473-482
18. Lee J.H., Sung Eun Park S.E., Lee H.J., Lee H.L.: Elsevier Materials Letters 56, 1022 (2002).
19. Kingery, W. D., J. Am. Ceram. Soc., Vol 38, N°1, 1955, pp. 3-15.